



LOMA LINDA UNIVERSITY

Loma Linda University  
TheScholarsRepository@LLU: Digital  
Archive of Research, Scholarship &  
Creative Works

---

Loma Linda University Electronic Theses, Dissertations & Projects

---

6-1995

## The Experimental Verification of the Efficacy of Finite Element Modeling to Dental Implant Systems

Thomas D. Baiamonte

Follow this and additional works at: <https://scholarsrepository.llu.edu/etd>



Part of the [Other Dentistry Commons](#)

---

### Recommended Citation

Baiamonte, Thomas D., "The Experimental Verification of the Efficacy of Finite Element Modeling to Dental Implant Systems" (1995). *Loma Linda University Electronic Theses, Dissertations & Projects*. 1296.  
<https://scholarsrepository.llu.edu/etd/1296>

This Thesis is brought to you for free and open access by TheScholarsRepository@LLU: Digital Archive of Research, Scholarship & Creative Works. It has been accepted for inclusion in Loma Linda University Electronic Theses, Dissertations & Projects by an authorized administrator of TheScholarsRepository@LLU: Digital Archive of Research, Scholarship & Creative Works. For more information, please contact [scholarsrepository@llu.edu](mailto:scholarsrepository@llu.edu).

ABSTRACT

THE EXPERIMENTAL VERIFICATION  
OF THE EFFICACY OF FINITE ELEMENT  
MODELING TO DENTAL IMPLANT SYSTEMS

BY

THOMAS D. BAIAMONTE, D.M.D.

The finite element method has previously been used to evaluate the stress distribution surrounding the dental implant to bone interface. However, prior finite element analysis models used have not been validated for the bone to implant interface. The objective of this study is to investigate whether the current Ansys finite element analysis model is an accurate biological representation of the observed clinical conditions. This will be accomplished by comparing data obtained experimentally of stress versus strain and the three dimensional computer generated finite element model.

The results indicate finite element method using the Ansys program for modeling is in agreement with the experimental stress strain plot and the calculated finite element data.

UNIVERSITY LIBRARY  
LOMA LINDA, CALIFORNIA

LOMA LINDA UNIVERSITY

Graduate School

---

THE EXPERIMENTAL VERIFICATION  
OF THE EFFICACY OF FINITE ELEMENT  
MODELING TO DENTAL IMPLANT SYSTEMS

by

THOMAS D. BAIAMONTE, D.M.D.

---

A Thesis in Partial Fulfillment  
of the Requirements for the Degree of Master of  
Science of Oral Implantology

---

June 1995

Each person whose signature appears below certifies that this thesis in their opinion is adequate, in scope and quality, as a thesis for the degree Master of Science.



\_\_\_\_\_, Chairperson

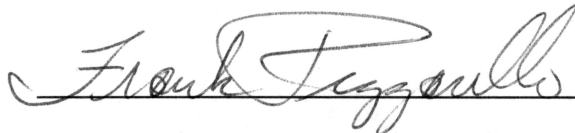
Jaime Lozada, Associate Professor of Restorative Dentistry



\_\_\_\_\_, Associate Professor of Restorative Dentistry



\_\_\_\_\_, Professor of Orthopedic Surgery



\_\_\_\_\_, Associate Professor

## ACKNOWLEDGEMENTS

Funding provided by Dentsply Corporation and Loma Linda University School of Dentistry.

TABLE OF CONTENTS

LIST OF FIGURES .....	v
LIST OF TABLES .....	vi
I. INTRODUCTION .....	1
II. MATERIAL AND METHODS .....	6
A. Animal Description .....	6
B. Implant Description .....	6
C. Expander, Abutment, and Implant Assembly .....	7
D. Experimental Data .....	11
E. Mathematical Analysis using Finite Element Method .....	15
III. DISCUSSION .....	19
IV. SUMMARY and CONCLUSION .....	21
V. REFERENCES .....	27

## LIST OF FIGURES

Figures	Page
1. Schematic View of Geometric Relationship of Implant Pair in Mandibular Section .....	9
2. Photographic View of Experimental Relationship ...	10
3. Experimental Data of Force versus Angular Displacement .....	12
4. Calculated Rigid Pivot Point versus Force .....	14
5. Sagittal View Superimposed Loaded and Unloaded FE Model .....	16
6. Sample Plot of Nodal Displacements in Y direction of Center Axis versus Distance from Apex to Top of Implant .....	18
7. Plot of Force versus Angular Displacement of Implant Pair - Second Run .....	20
8. Z Component of Stress Distribution Sagittal Section of Cortical Bone .....	23
9. Z Component of Stress Distribution Sagittal Section of Trabecular Bone .....	24

LIST OF TABLES

Table	Page
1. Comparison of Finite Element Calculations with Experimental Data .....	22

## INTRODUCTION

The stresses which are produced on implants when placed into function in the maxillary and mandibular bones are complex. They are comprised of compressional, torsional, and sheer stresses which vary topographically in magnitude and direction. An understanding of these stresses is important for the clinical application of dental implants as orthopedic anchors. The need to change a chemically and geometrically complex biological structure to a simpler geometric configuration with less complex physical properties is beneficial for the studying of stress distribution in the bone surrounding dental implants. This might be accomplished with the finite element method.

The first to achieve this finite dimensional procedure was Courant (1). He accomplished this by using a combination of variational formulations and sections of polynomial functions. This approach has since been successfully adopted by structural engineers (2), who call it the finite element procedure. The first introduction in the orthopedic literature of finite element (procedure) analysis method to analyze the mechanical behavior of bone was by Brekelmans (3).

The purpose of the paper is not to give a detail description of finite element method, but a brief description is pertinent. A general description of its principles, possibilities, and limitations in orthopedic biomechanical was published by Huiskes (4). The method is discussed in greater detail by Zienkiewicz (5).

When a structure is loaded, stresses are generated in its materials. The distribution of these stresses, their magnitudes and orientation throughout the structure, depend upon the loading configuration, the geometry of the structure, and the properties of the material. In addition, the stresses are influenced by the interaction of the structure at boundaries between different materials. In a stress analysis, the stress distribution is evaluated by using a mathematical model. In such a model, the structural aspects (load, geometry, material properties, boundary and interface conditions) are described mathematically. The mathematical descriptions are usually based on experimentally determined data. In the solution procedure, the structural descriptions are combined in mathematical equations based on theories of solid mechanics and these are solved to give the stresses.

Various theories and solution methods are available in classic mechanics for certain types of structures. The finite element analysis method, a computer method of structural stress analysis, is suitable in principle for any structure. Geometries, material properties, and complex loading are accounted for by the finite element analysis method.

In using the finite element method, a model as a geometric entity is defined first. This model is mathematically divided into a number of blocks, referred to as elements, connected at specific points called nodes. Every element is assigned one or more material properties.

Young's modulus and Poisson's ratio define its material properties. The computer program calculates the stiffness characteristics of each element and assembles the element mesh through mutual forces and displacement in each node. The finite element analysis method program solves a large number of equations that govern force equilibrium at element nodes.

The finite element model can be checked for accuracy by refining the element size and comparing the results obtained with the refined element size to the original element size. This is called a convergency test.

When interpreting the finite element method results, a differentiation between validity and accuracy of the model must be made. Accuracy of the model is the precision by which the finite element method mesh can approximate the exact solution for the model. Validation of the model is the precision by which the mathematical descriptions of structural aspects (load, geometry, material properties, boundary and interface conditions) simulates the actual structure. Only the accuracy can be verified with a convergency test, the validity must be verified by experimentation.

Recently, the finite element method has been used to determine the effect that the implant (6) and the implant-bone interface mechanical properties (7) has on the stress distribution of tissue surrounding dental implants. In addition, the finite element model has been used in the investigation of stress distribution pertaining to the

influence of implant shape differences, (8,9,10,11,12,13,14), implant diameter difference (15,16), material differences (17,18), treated verses non-treated implant surfaces (19,20,21), implants which contain and do not contain stress absorbing elements (22,23), and biomechanical properties (24,25,26,27,28,29,30,31,32,33). However, the results of the current two and three dimensional finite element models have not been validated.

A new method of generating finite element models of bone from computerized tomography scan data has been developed by Keyak (34). This method uses a contouring algorithm (35) to derive the bone geometry from the computerized tomography scan images. The finite element mesh generated is comprised of cube elements of a uniform size. Keyak (36) validated the accuracy of this finite element modeling technique through the comparison of strains predicted by this method with image strain measured on a human femur, in vitro. This method of computerized tomography scan images allows a rapid and accurate analysis do be done on the individual osseous system.

The central purpose of data presented here was to define the limit of compatibility of experimental data with a three dimensional finite element model created by the Ansys program (Swanson Analysis Systems, Inc., Houston, PA). This was accomplished by loading a pair of osseointegrated dental implants with known lateral forces and measuring the amount of displacement which occurred.

The experimental data was then compared to the data obtained from a compatible model generated in the Ansys program.

A loading device, (referred to as the expander) necessary to deliver the lateral forces, was designed and fabricated with the following characteristics:

- 1) the capacity of exerting lateral forces between paired dental implants.
- 2) exerting a range of verifiable forces.
- 3) provide a solid connection to the implant body.
- 4) removable from the implant pairs.

## MATERIALS AND METHODS

In this study, six hydroxylapatite coated titanium endosseous dental implants were placed in the mandible of a rhesus monkey. The technique for implantation followed the protocol recommended by the manufacturer (37). The mandibular bone was allowed to heal for two years. Within three hours of the animal's expiration, the mandible was retrieved, the soft tissue was removed, and the mandible was frozen. It was observed at the time of expiration that dehiscence of the gingival tissue over the implants was not present. The implants were connected to a loading device capable of applying a given amount of force. A pilot study was performed to develop a measuring technique and test the loading device.

### Animal

The animal was a twelve year old female rhesus monkey and weighed approximately twelve kilograms.

### Implants

The implants used were Bio Vent, 3.5mm diameter hydroxylapatite coated, purchased from Dentsply (formerly the Core-Vent Corporation). Implant lengths of 10.5mm and 13.0mm were used to form pairs.

### Expander, Abutment, and Implant Assembly

An expander device was fabricated of titanium and was of a scissor configuration with two blades and two handles. An expansion screw with a knurled nut at one end was placed between the two handles. This was used to apply a force at the blades by turning the knurled nut. Two strain gages were cemented, to specification by Vishay Co., to the handles of the expander. The magnitude of the force was sensed electronically by the the two strain gages. The pair of strain gages, used to sense the force, were connected to one leg of a Wheatstone Bridge circuit where a voltage imbalance was measured. The strain gages were calibrated by setting the loading blades of the expander equal to the distance between the implant abutments and then inserting the blades between a 1011 Instron head and anvil. The knurled nut was turned to yield an imbalance voltage related to a force read from the Instron. This procedure produced a reproducible calibration curve capable of measuring force to an accuracy of  $\pm 0.001$  Newton. To achieve this level of accuracy, temperature compensated alloy strain gages made by the Vishay Co. were used. The unbalanced voltage was measured using a digital volt meter accurate to  $\pm 1 \times 10^{-6}$  volts.

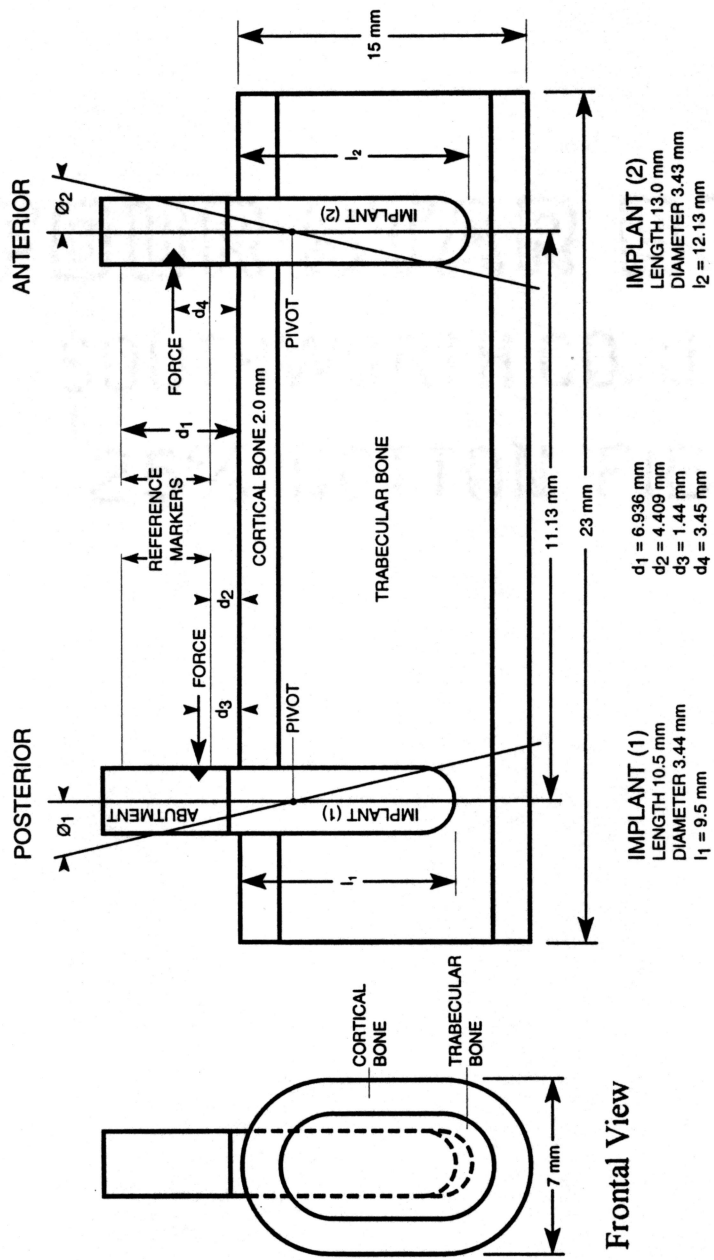
Two abutments were cast from PG200 alloy. The abutment had a male interlocking hex design which mated with the female internal hex design of the implant. The hex design was utilized to prevent rotation of the abutment within the

implant. Each abutment casting had one notch on the medial surface to precisely engage one blade of the expander. In addition, each abutment had two reference markers used to measure distance. They were placed at different heights parallel to the long axis and cemented to the abutment with cyanoacrylate. The abutment was fixed to the implant by means of an abutment screw which was torqued to 30 Newton centimeters.

The mandible was passively fixed along the inferior border on a rigid plate with polymethylmethacrylate.

Figure 1. shows a schematic view of the dimensional relationships of the implant pair in the mandible section investigated. Figure 2 shows a photographic view of the experimental arrangement. This photo shows the expander set in position against the abutments. The expander device was used to apply a known spreading force between abutments by turning the knurled nut shown. At each succeeding change of force the resulting displacements were measured. The application of the force was made at points above the mandibular crest, thus producing a rotational motion at each of the implants. To define the angular displacements of the implants it was necessary to measure the linear change of length between the abutments at two vertical positions along the length of the abutments. The displacements were measured between the reference points shown in Figure 1 and 2 using a traveling microscope accurate to  $\pm 1$  micron.

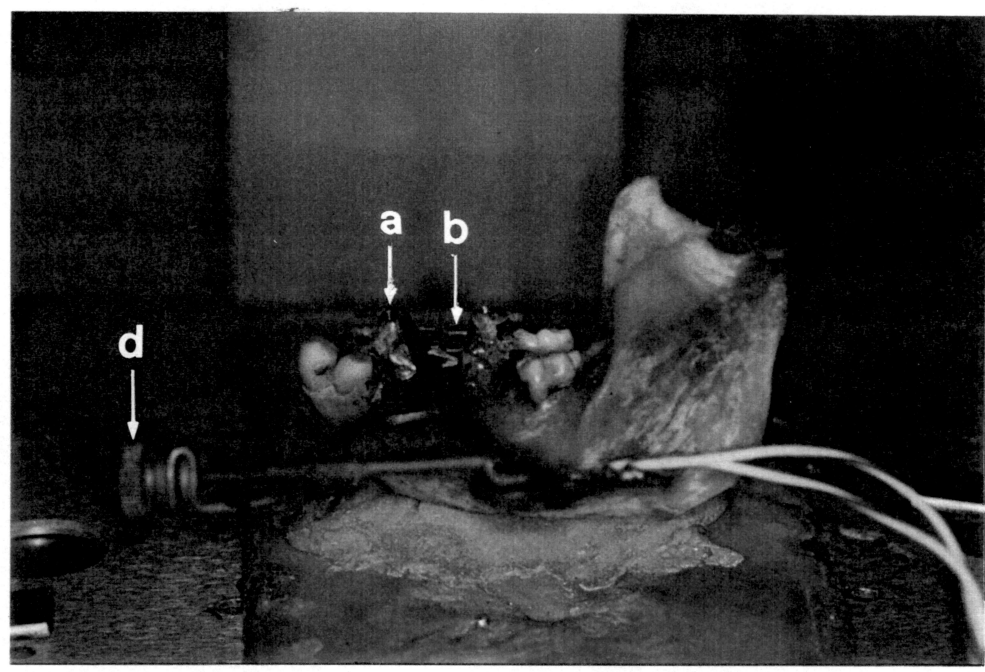
Since the expander was built in the configuration of a scissor a mechanical advantage exists between the long



Sagittal View

Figure 1 Schematic View of Geometric Relationship of Implant Pair in Mandibular Section

A: Sagittal View



B: Top View

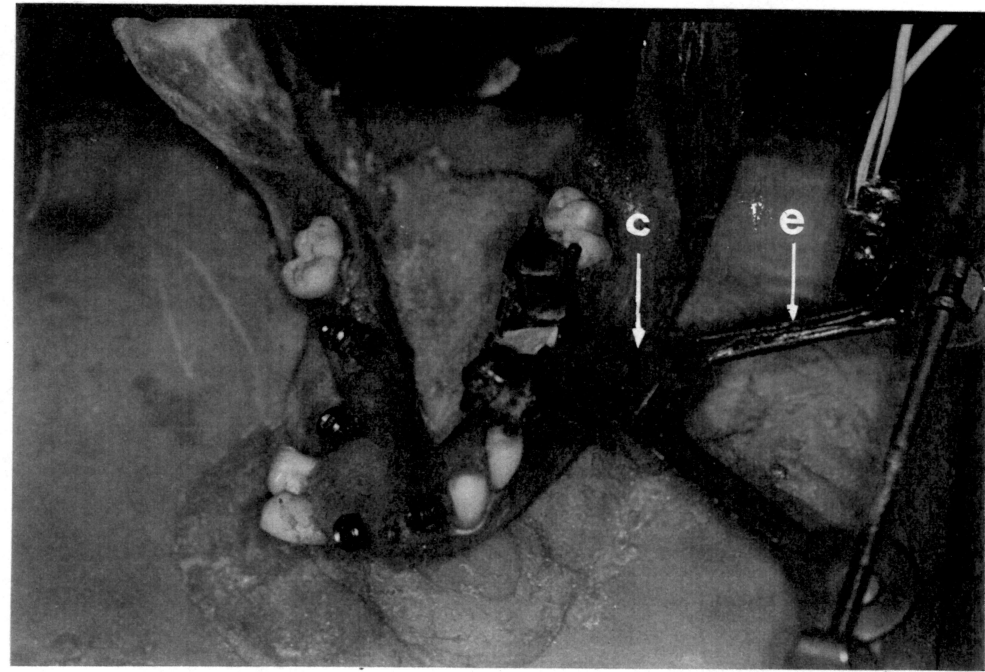


Figure 2 Photographic View of Experimental Arrangement

- Legend:      a. Abutment    b. Reference Marker    c. Expander  
                 d. Knurled nut    e. Strain Gage

handles holding the knurled nut/expansion screw mechanism and the short blades. The mechanical advantage of the expander is four; thus a great deal of force can be exerted at the blades. Forces as high as 245 Newton were achieved with the expander in the pilot study. However, a mechanism of a mechanical advantage of four requires a precise placement of the loading blades against the abutment surface to achieve a reproducible force. During the calibration of the strain gages, the same points on the loading blade should be used against the anvil and head of the Instron as the abutments. These requirements were met by casting mating surfaces on the abutment medial surface and the calibration jig fixed to the Instron.

#### Experimental Data

Figure 3 gives a plot of the experimental data as angular displacement verses the force. The angular displacement given on this graph was calculated using linear displacement data from the abutment reference markers measured with a traveling microscope. Using the geometry shown in Figure 1, a trigonometrical relation was derived for the angular displacement in terms of the linear distances measured. The relation giving the total angular displacements between the implants is:

$$\theta(T) = \arcsin\{[dx(t) - dx(b)]\} / [d(1) - d(2)] \quad (1)$$

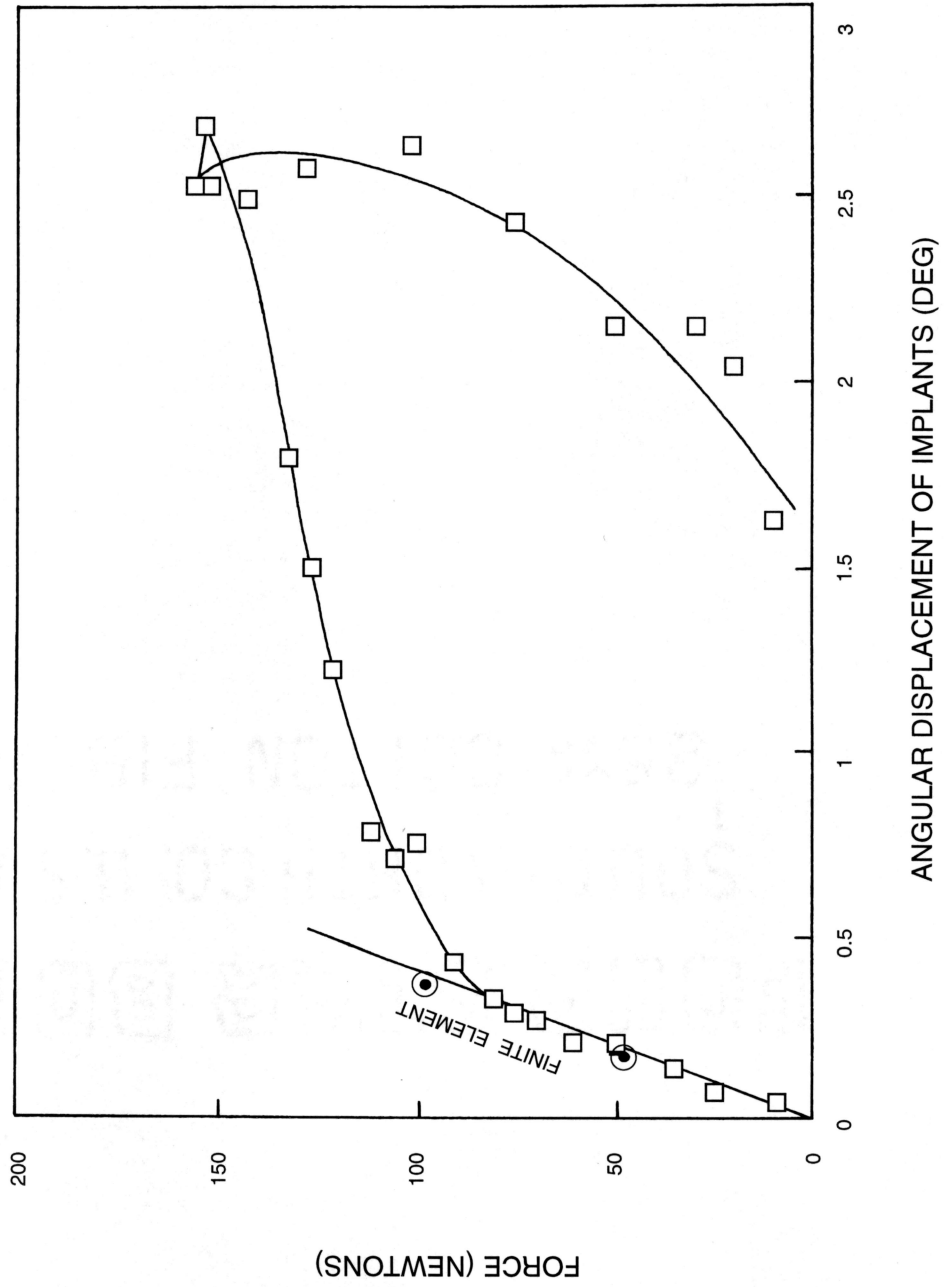


Figure 3 Experimental Data of Force versus Angular Displacement

where,  $dx(t)$  is the linear displacement measured at the top of the reference markers,  $dx(b)$  is the linear displacement of the bottom of the reference markers.  $d(1)$  and  $d(2)$  are the heights of the reference markers above the mandibular crest shown in Figure 1. In general, it is expected that each implant will rotate at different angles because the implants are of a different length and the force is applied at different positions on the abutments. Thus equation 1 gives the total angle  $\Theta(T)$  which is the sum  $\Theta(1)$  and  $\Theta(2)$ .

$$\Theta(T) = \Theta(1) + \Theta(2) \quad (2)$$

Figure 4 gives a plot of the pivot points with increasing force. The angular displacements plotted in Figure 3 imply a rotational motion of the implants. The center of rotation is the pivot point and is defined as the axis about which rotation takes place on the center line of the implant structure. The pivot point is calculated by the relationship:

$$P = d(1) - [dx(t) / 2\sin\Theta(T)] \quad (3)$$

This relationship is derived with the assumption that the titanium implants are rigid bodies and pivot through the contacting bone structure, when loaded, without bending. Negative values of  $P$  in equation 3 give the distance below the mandibular crest.

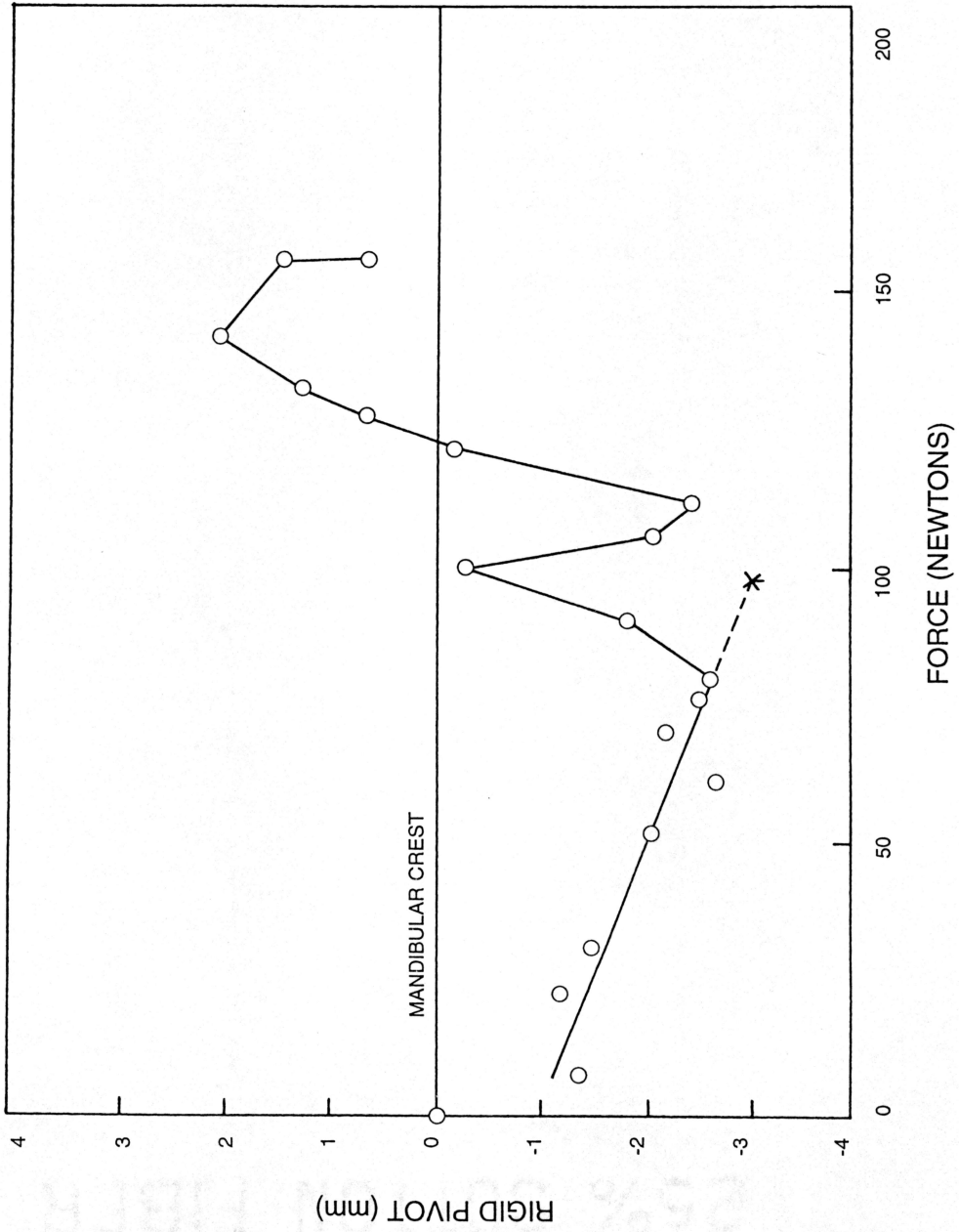


Figure 4 Calculated Rigid Pivot Point versus Force

### Mathematical Analysis using Finite Element Method

The finite element three dimensional model was composed by entering into the Ansys finite element program keypoint data from CAT scan of the mandible of a macaca monkey. The section of mandible used was of regular geometry requiring 24 keypoints to produce a good representation of the actual mandible in three dimensions.

A sagittal view of a finite element model generated for the section of the mandible is given in Figure 5. This Figure shows the displacements as superimposed on the loaded and unloaded model. The model generate contains 10,000 nodes and 10,000 tetrahedral solid elements. The boundary conditions imposed to simulate the strain produced in the actual experimental mandible was to mechanically restrain the bottom nodes of the model in all coordinate directions. This configuration of restraint was compatible with the actual mandible fixed along the inferior border on a rigid plate with polymethylmethacrylate during loading by the expander. The Young's modulus of the material used are: Titanium  $1.07 \text{ E}5 \text{ N/sqmm}$ , cortical bone  $1.72 \text{ E}4 \text{ N/sqmm}$ , and trabecular bone  $2.22 \text{ E}3 \text{ N/sqmm}$  (38). The Poisson's ratio used for all materials was .33. An alternate method of restraint was also imposed as a boundary condition to the model where the opposite ends of the mandibular section was restrained in all coordinate directions. This alternated boundary condition was investigated since a complete mandible was measured extending beyond the dimensional

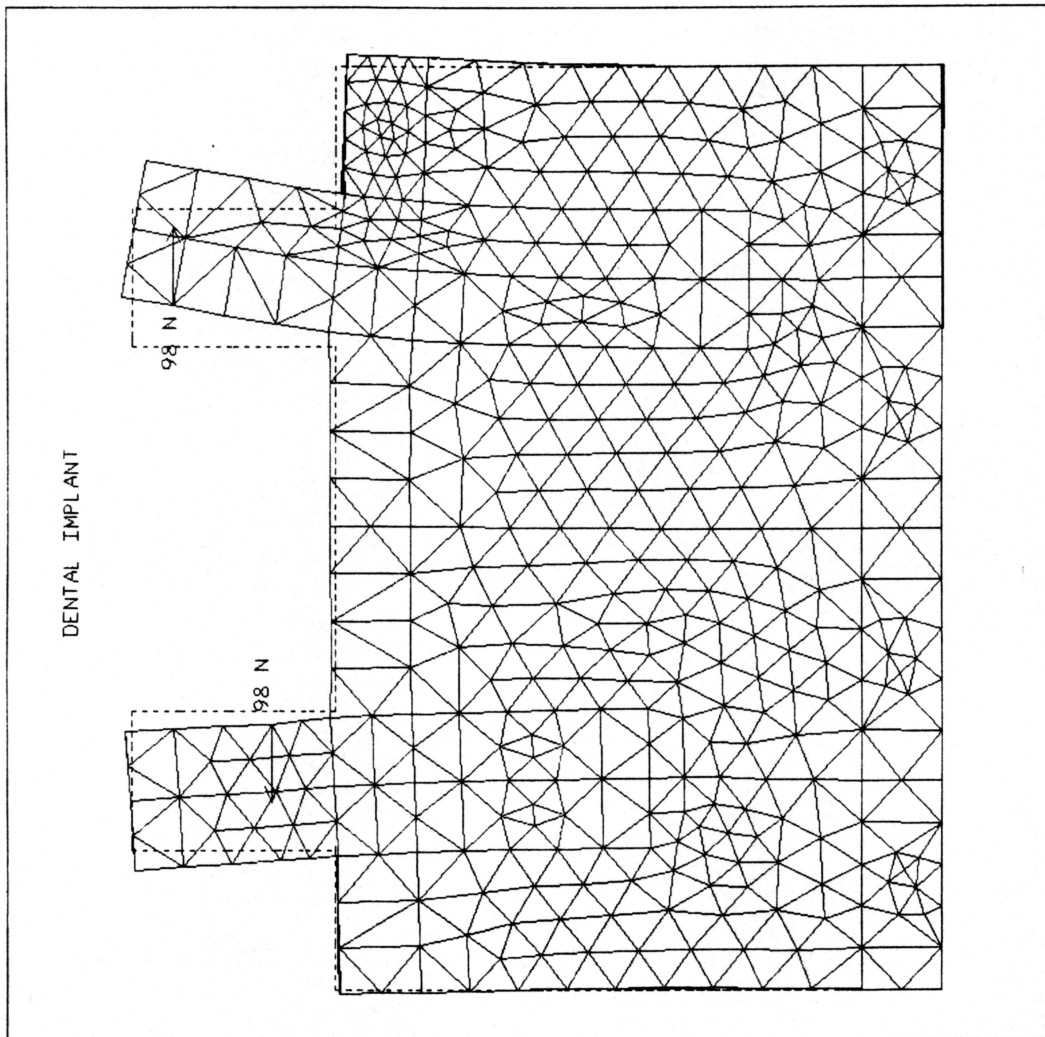


Figure 5 Sagittal View Superimposed Loaded and Unloaded FE Model

limits imposed by the model. The results of the two restraint cases is given in Table 1. Figure 5 also shows the position along each abutment where the force was applied and the resulting displacements. Unlike the assumption made in the derivation of equation 2 that the implant and abutment are rigid bodies, the finite element method calculations show the deformations of the implants and mandible section.

Figure 6 is a sample of the data obtained, where the load modulus and restraint were changed, showing a plot of the implant centerline y axis nodal displacement component as a function of the vertical z axis distance from the apex of an implant. Note that at the abutment portion above the ridge of the displacement is essentially linear. Approaching the cortical ridge and through the ridge a pronounced bending of the implant occurs. The curve continues through zero displacement at some distance from the apex and at the apical end of the implant shows a negative displacement. The negative displacement calculated in Figure 6 is the motion of the implant apex through the bone structure. The point of intersection of the zero displacement line with the curve gives the true pivot and the intersection of the extrapolated linear portion of the curve with the zero line gives the rigid pivot which is related to the pivot calculated by equation 3 and given in Figure 4. The slope of the linear portion of the curve in Figure 6 is the  $\tan\theta$  of the angular displacements of either implant 1 or 2. The sum of these angular displacements

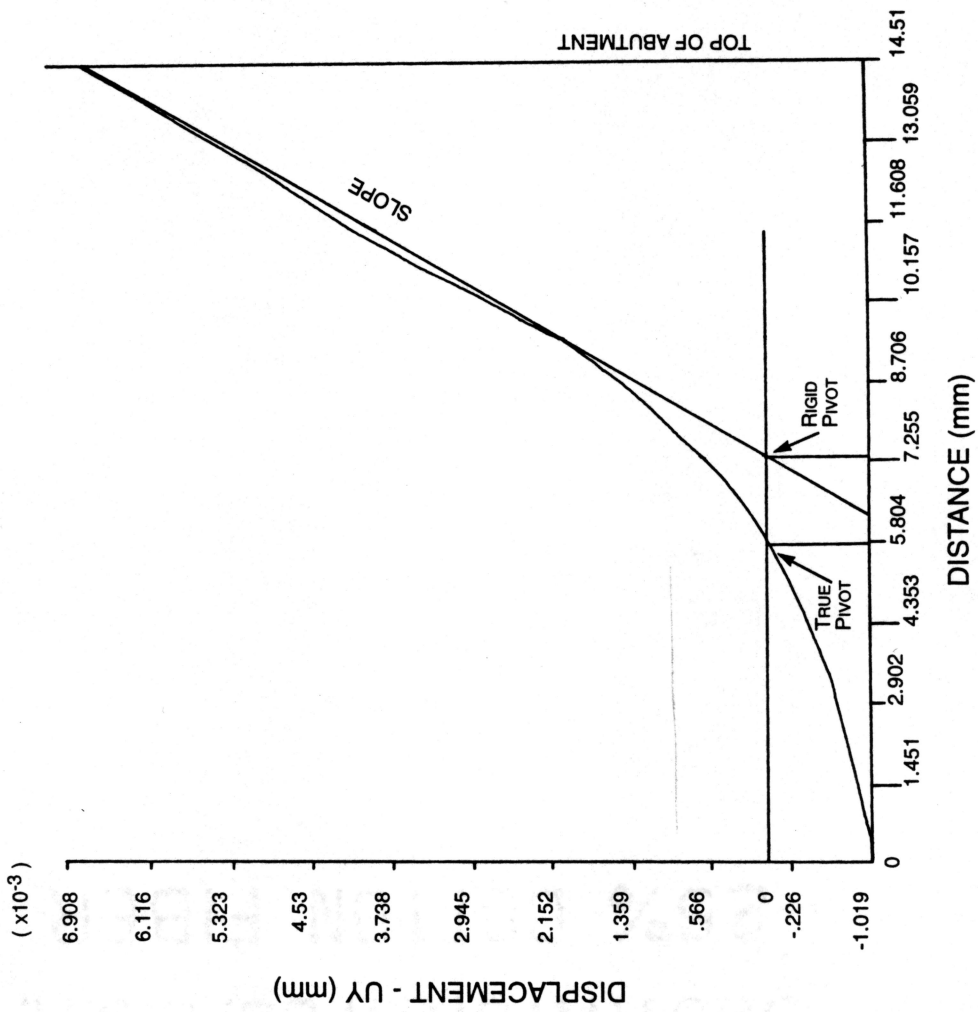


Figure 6 Sample Plot of Nodal Displacement in Y Direction of Center Axis versus Distance from Apex to Top of Abutment

calculated from the slope of the curves for implant 1 and 2 equals the total angular displacement  $\Theta(T)$ .

### Discussion

Three regions of interest are shown in Figure 3; first a linear portion in the range of forces starting at zero and ending at approximately 88N; second an abrupt knee with a curve portion moving from 88N to 147N; and third a curve departing from the ascending curve as the force is reduced. The linear regions shown in Figure 3 and 4 is interpreted as the bone acting elastically (39). Experimentally, this elastic behavior was noted by checking the reversibility of the displacement by increasing and decreasing the force over a small range. In the second region shown in Figure 3, it is believed that a relaxation phenomena has occurred in the surrounding bone structure. Figure 4 contributes to this conclusion by showing the onset of a change in the bone structure at forces greater than 88N by the wide variations noted in the pivot point. The third and final region where irreversibility is observed is further evidence of damage to bone structure surrounding the implant. Figure 7 shows the force versus angular displacement curve of the same implant pair remeasured. Note that the curve is no longer smooth but oscillates between higher and lower values of angular displacements as the force is increased. These data are given as further evidence of a relaxation process that has occurred in the bone structure surrounding the implant. The

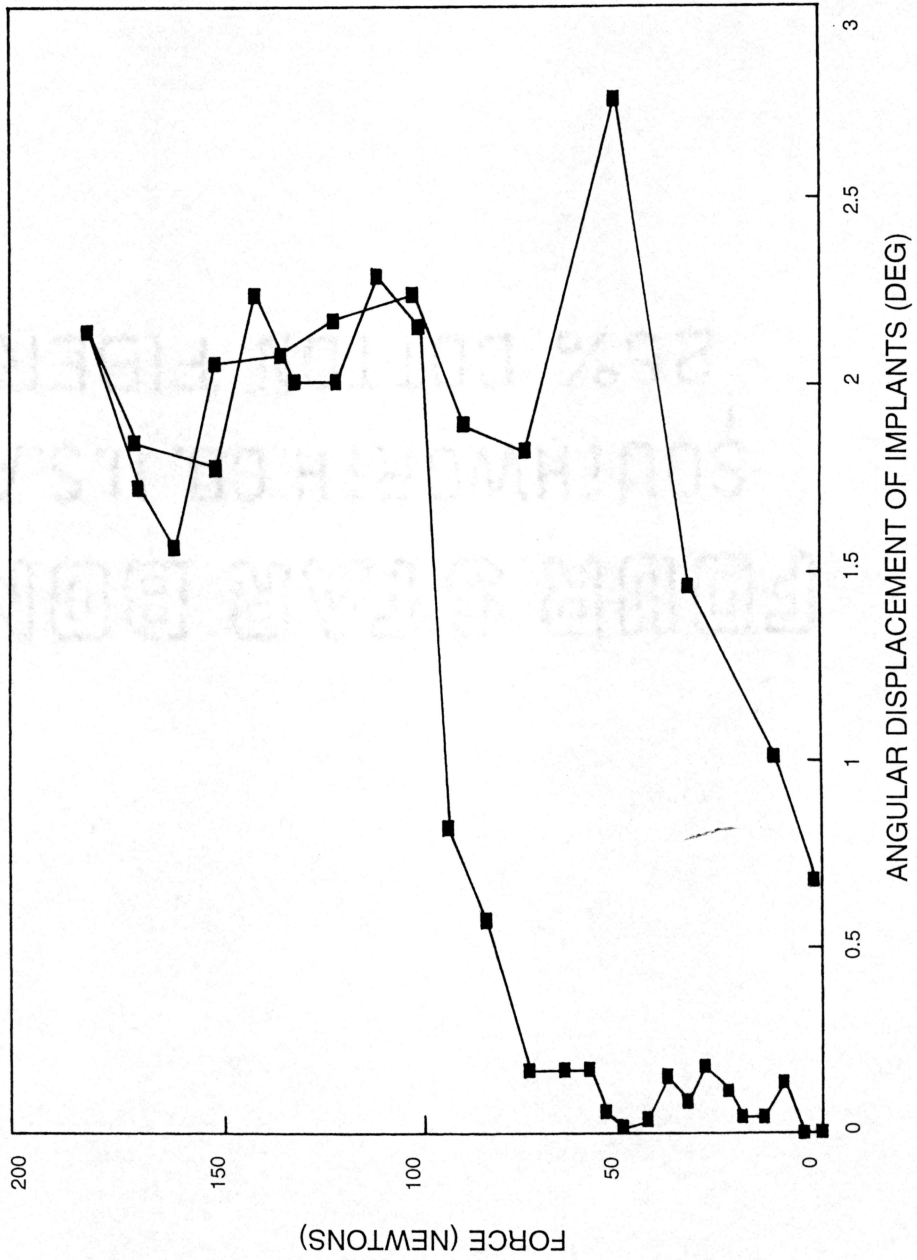


Figure 7 Plot of Force versus Angular Displacement of Implant Pair - Second Run

extent of damage was not determined in these experiments. It is speculated that if living tissue was used in these experiments, restoration of the bone structure might occur with time. This would be evidenced by measurements of stress strain data after time, noting the reestablishment of a linear curve similar to the first region in Figure 3.

Table 1 summarizes the finite element data calculated and compares these data experimentally. The table presents the finite element data for several cases for each restraint boundary condition: one, where the literature value of the Young's modulus for the trabecular bone of  $2.2 \text{ 3N/sqmm}$  is used and where the test value of  $1.1 \text{ 3N/sqmm}$  is used, and two, where the applied force values of 49N and 98N were used. Table 1 gives the values of the true pivot of implant 1 and 2, and the rigid pivot of implant 1 and 2 calculated from the finite element method and the angular displacements of the individual implants.

Figures 8 and 9 are presented to show the additional information obtained from the model which can not be obtained experimentally. These figures show the shear stress intensity distribution for 98N of a sagittal section of the mandible. Figure 8 shows sagittal section of the cortical bone shell. Figure 9 is a sagittal section of the interior trabecular bone.

FEM CALCULATIONS						EXPERIMENTAL DATA		
LOAD	MODULUS	TRUE PIVOT	RIGID PIVOT	ANGLE		LOAD	RIDGE PIVOT	ANGLE $\phi_T$
N	N/MM <sup>2</sup>	MM P(1) P(2)	MM P(1) P(2)	DEG $\phi(1) \phi(2)$		N	MM	DEG
MECHANICAL RESTRAINT AT BOTTOM OF THE SECTION								
49	1.1E3	-3.36 -5.07	-2.13 -1.99 P <sub>AV</sub> -2.06	.057 .156 $\phi_T$ =.213		49	-2.0	0.20
49	2.2 E3	-3.70 -7.58	-2.25 -1.93 P <sub>AV</sub> -2.09	.050 .114 $\phi_T$ =.194				
98	1.1 E3	-3.36 -6.54	-2.08 -2.03 P <sub>AV</sub> -2.05	.122 .301 $\phi_T$ =.423		98	-3.0	0.39
98	2.2 E3	-4.20 -7.06	-3.30 -1.93 P <sub>AV</sub> -2.62	.100 .287 $\phi_T$ =.387				
MECHANICAL RESTRAINT ON SIDES OF THE SECTION								
49	2.2 E3	-4.03 -3.24	-2.07 -0.95 P <sub>AV</sub> -1.15	.047 .129 $\phi_T$ =.176		49	-2.0	0.20
98	2.2 E3	-4.26 -3.24	-2.13 -0.95 P <sub>AV</sub> -1.54	.098 .260 $\phi_T$ =.36		98	-3.0	0.39

Table 1  
Comparison of FEM Calculations with Experimental Data

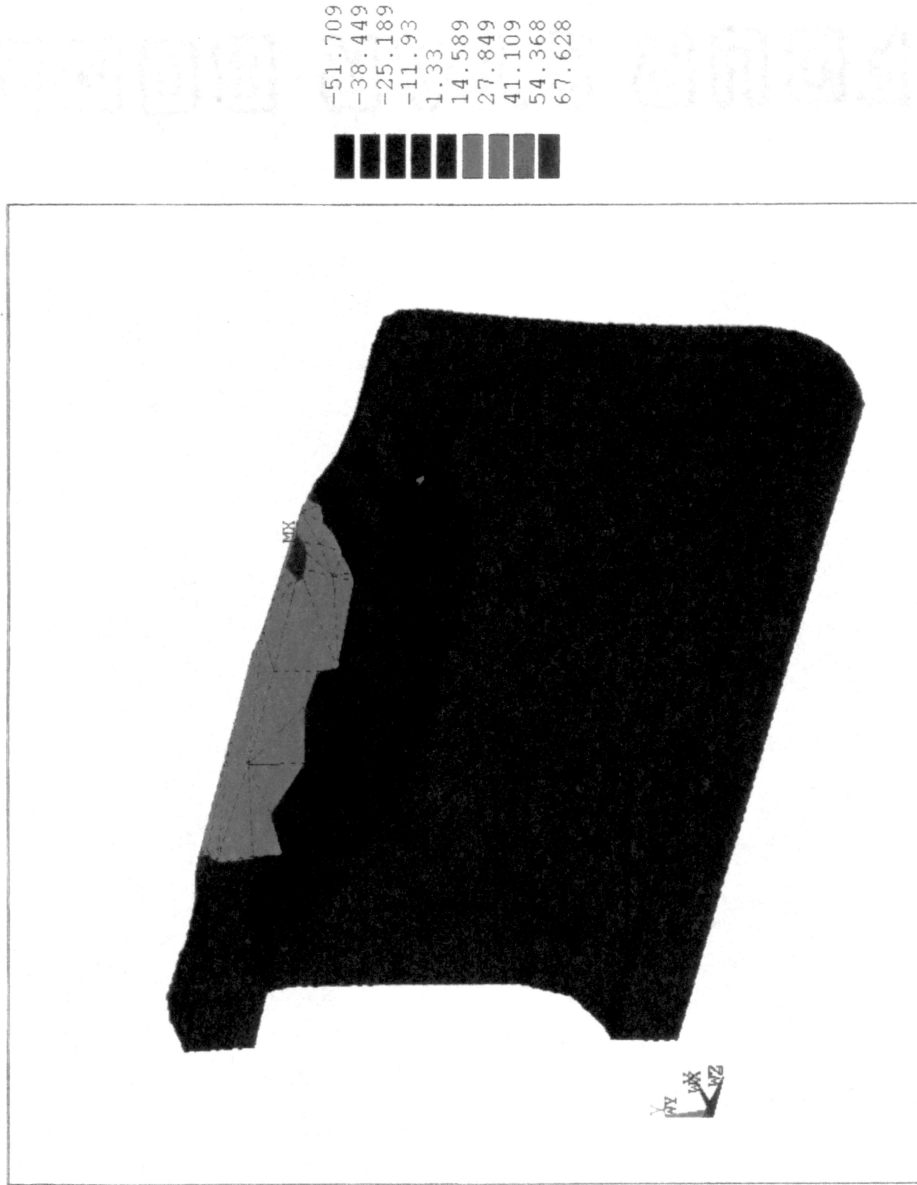


Figure 8 Z Component of Stress Distribution:  
Sagittal Section of Cortical Bone

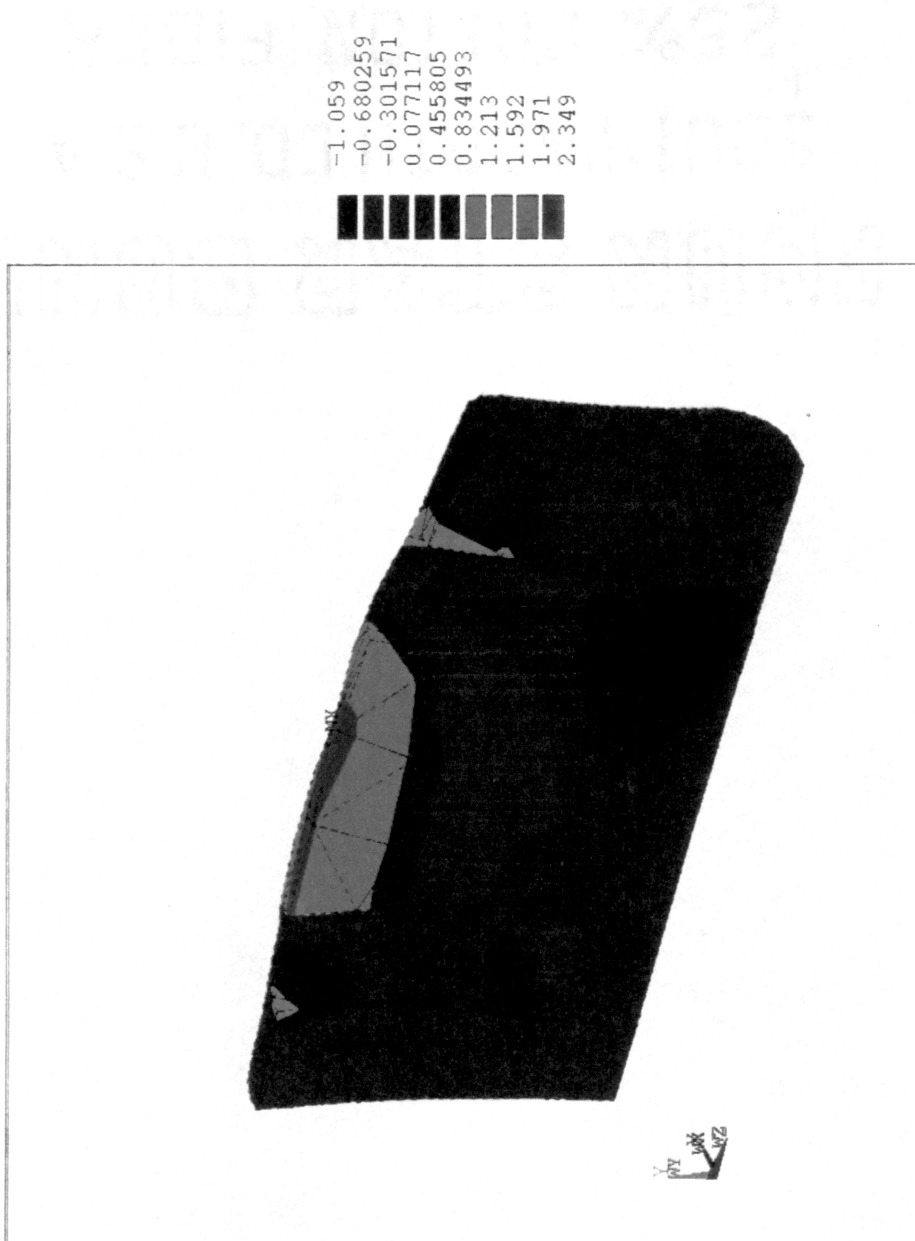


Figure 9 Z Component of Stress Distribution:  
Sagittal Section of Trabecular Bone

### Summary and Conclusion

From the data presented a number of conclusions can be drawn. First, both experimental data and finite element model show the angular displacement is linear with force and the pivot point moves down through the implant from the mandibular crest with increasing force. Second, the experimental angular displacements are only 3% less than the angular displacements calculated by the finite element model. Agreement to this extent is better than expected since the distance measurements had a precision of  $\pm 1$  micron, which at the lower forces, gives displacement errors as high as 10%. At higher forces the precision increases to less than 5%. The agreement calculated for the pivot also was good, showing a deviation of the finite element rigid pivot of between 5% and 13% from the experimental values at 49N and 98N. Third, the finite element model gives a complete view of the displacements of the implants on static loading, including bending of the implants. Data of this kind can have practical clinical implications. Fourth, the literature values of the modulus of elasticity for the cortical and the trabecular bone are sufficiently accurate to be used for finite element calculation of models of the mandible. The data of table 1 shows an average 12% increase of elasticity in the angular displacement when the trabecular bone modulus is decreased by a factor of two. Intuitively, an increase in the angular displacement is expected when the modulus of elasticity of the trabecular

bone is decreased and is verified by the finite element calculations. Finally, the comparative data verifies the actual physical structure of the implant. It is held firmly by the cortical ridge bone, with the lower portion of the implant embedded and held in the softer interior trabecular bone of the mandible.

## REFERENCES

1. Courant, R., "Variational Methods for the Problem of Equilibrium and Vibrations" Bull. Amer. Math. Soc. 1943; 49: 1-23
2. Turner, M.J., Clough, R.W., Martin, H.C., Topp, L.J., "Stiffness and Deflection Analysis of Complex Structures" J. Aero. Sciences 1956; 23
3. Brekelmans, W.A., Poort, H.W., Shoff, T.J., "A New Method to Analyze the Mechanical Behavior of Skeletal Parts" Acta Orthop. Scand 1972; 43: 301-317.
4. Huiskes, R., "Principles and Methods of Solids Biomechanics Functional Behavior. Functional Behavior of Orthopedic Biomaterials Vol. I. Fundamentals" Boca Raton, FL: CRC Press, 1983
5. Zienkiewicz, O.C., "The Finite Element Method" Third ed. London: McGraw-Hill, 1977
6. Cook, S.D., Klawitter, J.J., Weinstein, A.M., "The Influence of Implant Elastic Modulus on the Stress Distribution Around LTI Carbon and Aluminum Oxide Dental Implants" J. Biomed. Mater. Res. 1981 Nov.; 15(6): 878-887.
7. Lavernia, C.J., Cook, S.D., Weinstein, A.M., Klawitter, J.J. "The Influence of the Bone-Implant Interface Stiffness on Stress Profiles Surrounding Al2O3 and Carbon Dental Implants" Ann. Biomed. Eng. 1982; 10(3): 129-138.
8. Siegele, D., Soltesz, U., "Numerical Investigations of the Influence of Implant Shape on Stress Distribution in the Jaw Bone" Int. J. Oral Maxillofac. Implants 1989 Winter; 4(4): 333-340.
9. Rieger, M.R., Mayberry, M., Brose, M.O., "Finite element Analysis Of Six Endosseous Implants" J. Prosthetic Dent. 1990 June; 63(6): 671-676.
10. Rieger, M.R., Adams, W.K., Kinzel, G.L., "A Finite Element Survey of Eleven Endosseous Implants" J. Prosthetic Dent. 1990 April; 63(4): 457-465.
11. Mihalko, W.M., May, T.C., Kay, J.F., Krause, W.R., "Finite Element Analysis of Interface Geometry Effect on the Crestal Bone Surrounding a Dental Implant" Implant Dent. 1992 Fall; 1(3): 212-217.

12. Cook, S.D., Weinstein, A.M., Klawitter, J.J.,  
"Parameters Affecting the Stress Distribution Around  
LTI Carbon and Aluminum Oxide Dental Implants" J.  
Biomed. Mater. Res. 1982 Nov.; 16(6): 875-885.
13. Cook, S.D., Klawitter, J.J., Weinstein, A.M., "The  
Influence of Implant Geometry on the Stress  
Distribution Around Dental Implants" J. Biomed.  
Mater. Res. 1982 July; 16(4); 369-379.
14. Lozada, J.L., Abbate, M.F., Pizzarello, F.A.,  
James, R.A., "Comparative Three-Dimensional Analysis  
of Two Finite Element Endosseous Implant Designs"  
J. Oral Implantol. 1994; 10(4): 315-321.
15. Matsushita, Y., Kito, M., Mizuta, K., Ikeda, H.,  
Suetsugu, T., "Two Dimensional FEM Analysis of  
Hydroxyapatite Implants: Diameter Effects on Stress  
Distribution" J. Oral Implantol. 1990; 16(1): 6-11.
16. Katayama, T., Takuma, M., Morimoto, K., Nakamura, S.,  
Takashima, F., Maruyama, T., "Stress Analysis of  
Titanium-Hydroxyapatite Implant. Effect of Titanium  
Diameter on Reinforcement and Calculation of Implant  
Diameter" Nippon Hotetsu Shikagakkai Zasshi  
1990 Feb.; 34(1): 191-196.
17. Nishihana, K., Nakagiri, S., "Biomechanical Studies on  
Newly Tailored Artificial Dental Roots"  
Biomed. Mater. Eng. 1994; 4(3): 141-149.
18. Takuma, M., Tsutsumi, S., Tsukamoto, H., Kimura, Y.,  
Fukunaga, S., Takamori, Y., "The Influence of  
Materials Difference on Stress Distribution and Bone  
Remolding Around Alumina and Titanium Dental  
Implants" J. Osaka Univ. Dental School 1990 Dec.;  
30: 86-96.
19. Reiger, M.R., Adams, W.K., Kinzel, G.L., Brose, M.O.,  
"Finite Element Analysis of Bone Adapted and Bone  
Bonded Endosseous Implants" J. Prosthe. Dent. 1989  
Oct.; 62(4): 436-440.
20. Cook, S.D., Klawitter, J.J., Weinstein, A.M., "A Three  
Dimensional Finite Element Analysis of a Porous  
Rooted Co-Cr-Mo Alloy Dental Implant" J. Dent. Res.  
1982 Jan.; 61(1): 25-29.
21. Cook, S.D., Weinstein, A.M., Klawitter, J.J., "A Model  
for the Implant-Bone Interface Characteristics of  
Porous Dental Implants" J. Dent. Res. 1982 Aug.;  
61(8): 1006-1009.

22. van Rossen, I.P., Braak, L.M., dePutter, C., deGoot, K., "Stress Absorbing Element in Dental Implants" J. Prosthe. Dent. 1990 Aug.; 64(2): 198-205.
23. Holmes, D.C., Grigsby, W.R., Goel, V.K., Keller, J.C., "Comparison of Stress Transmission in the IMZ Implant System with Polyoxymethylene or Titanium Intramobile Element: A finite Element Stress Analysis" Int. J. Oral Maxillofac. Implants 1992 Winter; 7(4): 450-458.
24. Nishihara, K., Nakagiri, S., "Biomechanical Research on Junction System of Bone with Biomaterials" Biomed. Mater. Eng. 1994; 4(3): 151-159.
25. Meijer, H.J., Starmans, F.J., Steen, W.H., Bosman, F., "A Three Dimensional Finite Element Study on Two Versus Four Implants in an Edentulous Mandible" Int. J. Prosthodont. 1994 May-June; 7(3): 271-279.
26. Clelland, N.L., Lee, J.K., Bimbenet, O.C., Gilat, A., "Use of an Axisymmetric Finite Element Element Method to Compare Maxillary Bone Variables for a Loaded Implant" J. Prosthodont. 1993 Sept.; 2(3): 183-189.
27. Meijer, H.J., Starmans, F.J., Steen, W.H., Bosman, F., "A Three Dimensional Finite Element Analysis of Bone Around Dental Implants in an Edentulous Human Mandible" Arch. Oral Biol. 1993 June; 38(6): 491-496.
28. Clift, S.E., Fisher, J., Watson, C.J., "Finite Element Stress and Strain Analysis of the Bone Surrounding a Dental Implant: Effect of Variations in the Bone Modulus" Proc. Inst. Mech. Eng. H. 1992; 206(4): 233-241.
29. Meijer, H.T., Starmans, F.J., Bosman, F., Steen, W.H., "A Comparison of Three Finite Element Models of an Edentulous Mandibles Provided with Implants" J. Oral Rehabil. 1993 Mar.; 20(2): 147-157.
30. Meijer, H.T., Kuiper, J.H., Starmans, F.J., Bosman, F., "Stress Distribution Around Dental Implants: Influence of Superstructure, Length of Implant, and Height of Mandible" J. Prosthe. Dent. 1992 July; 68(1); 96-102.
31. Ko, C.C., Kohn, D.H., Hollister, J.J., "Micromechanics of Implant Tissue Interfaces" J. Oral Implantol. 1992; 18(3): 220-230.

32. Clelland, N.L., Ismail, Y.H., Zaki, H.S., Pipko, D.,  
"Three Dimensional Finite Element Analysis in and  
Around the Screw-Vent" Int. J. Oral Maxillofac.  
Implants 1991 Winter; 6(4): 391-398.
33. Gieloff, B., Kanth, L., "Implant Optinization with Help  
of Numerical Finite Element Studies" ZWR 1991 Nov. ;  
100(11): 860-863.
34. Keyak, J.H., Meagler, J.M., Skinner, H.B., Mote, C.D.  
Jr., "Automated Three Dimensional Finite Element  
Modelling of Bone: A New Method" J. Biomed. Eng.  
1990; 12: 389-397.
35. Seitz, P., Ruegsegger, P., "Fast Contour Detection  
Algorithm for High Precision Quantitative CT" IEEE  
Trans. Med. Imag. 1983; MI-2(3): 136-141.
36. Keyak, J.H., Fourkas, M.G., Meagher, J.M., Skinner,  
H.B., "Validation of an Automated Method of Three  
Dimensional Finite Element Modelling of Bone" J.  
Biomed. Eng. 1993; 15: 505-509.
37. Core-Vent Corporation, "Surgical Protocol for BioVent  
Implant" 1989.
38. Bidez, M.W., Stephens, B.J., Lemonds, J.E., "An  
Investagation into the Effect of Blade Dental  
Implant Length on IInterfacial Tissue Stress  
Profiles" Comput. Meth. Bioeng. 1988;11-17-12-2:  
235-243.
39. Fung, Y.C., "Biomechanics: Mechanical Properties of  
Living Tissue" Second ed. Springer-Verleg New York  
1993;510-513.